Supplementary materials

S1 Particle size distributions of the starting raw materials.

Optical parameters for PC were n = 1.73 and k = 0.1. For the NFM slag the refractive index was determined as 1.72 using the Gladstone-Dale model with values as tabulated by Young and Finn [1], and the imaginary coefficient k was taken similar to PC (0.1) as this did not yield an overly large fraction of submicron particles and thereby deemed acceptable. The resulting particle size distributions are shown in figure Sf1.

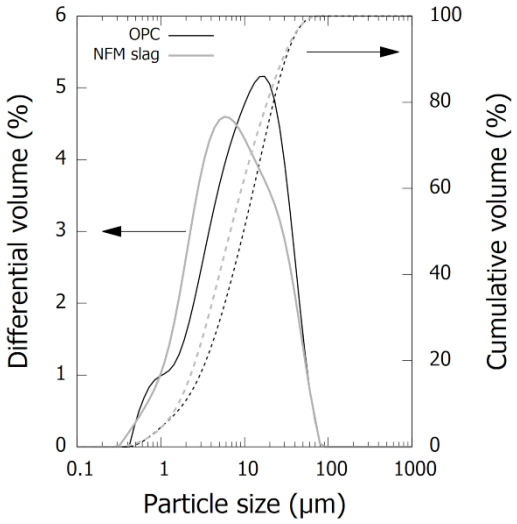

Figure Sf1 differential and cumulative particle size distribution of the raw materials.

S2: Description of the Quantitative X-ray diffraction strategy and crystal structures.

For the anhydrous Portland cement quantification a 5th order Chebychev function combined with a 1/x term was used in order to fit any X-ray amorphous phases. On the other hand the amorphous part of the slag was fitted using an Pawley phase ('hkl_Is' in Topas). This Pawley phase was later used in the "partial or no known crystal structure" (PONKCS) method [2] in order to determine the residual unreacted slag content of the hydrated cement blends. The procedure was similar to that used and described by Li et al. [3] for the quantification of amorphous siliceous fly ash in hydrated blended cements. As background a zero-order Chebychev function was used combined with a 1/x term. The calcium-silicate-hydrate (C-S-H) structure was modelled using 4 reflections based on a 7-year old white cement, as described by Li et al. [3]. Additionally, the position, intensity and crystallite size of the major reflection at a d-spacing of 3.03 Å (originally) was refined based on the patterns of each blended cement at 150 days in order to get a profile that is more representative of the C-(A)-S-H structure in those blends. The result obtained using this refined C-(A)-S-H structure is reported in the main text. Both the results based on the original C-S-H structure of 7-year old white cement and the refined structure described before are reported and discussed below in the supplementary materials S5. Finally, the main reflection due to the unidentified phase discussed in the main text, was accounted for using a single peak ('d_Is' in Topas) with constrained Lorentzian crystallite size peak broadening at the relevant d-spacing (7.4 ± 0.05). This does not account for any other peaks present corresponding to this phase and will thus lead to a certain error which at this point cannot be accounted for.

Table St1: Crystal structures used in the Rietveld analysis.

Phase	Reference

C_3S M3	[4]
C_3S M1	[5]
C_2S-β	[6]
C_2S-α'	[7]
C_3A cubic	[8]
C_3A orthorhombic	[9]
C_3A monoclinic	[10]
C_4AF	[11]
Anhydrite	ICDD-371496
Bassanite	ICDD-410224
Gypsum	ICDD-360432
Calcite	ICDD-50586
Dolomite	ICDD-360426
Quartz	ICDD-331161
Periclase	ICDD-450948
Syngenite	ICDD-280739
Aphthitalite	ICDD-200928
Lime	ICDD-371497
Portlandite	[12]
Ettringite	[13]
Hemicarboaluminate	[14]
Carbonated hemicarboaluminate	[14]
Monocarboaluminate	[15]
Hydrotalcite Mg/Al = 2	[16]
Siliceous hydrogarnet	[17]
Calcium-Silicate-Hydrate	[3]

S3: The composition of the solution and the parameters of the selective dissolution procedure.

Table St2: Parameters for the selective dissolution procedure.

Solution	**Volume ratio**
0.05 M 2Na-EDTA, 0.1 M NaOH mixture	10
H_2O	10
1:1 TEA:H_2O mixture	1
1 M NaOH	2.5
Parameters	
Weight powder	0.25 g
Volume solution	293.75 ml (1175 ml/g)
Time	30 min
Stirring rate	200 rpm
Washing liquids	H_2O, ethanol
Pre- & post-drying T (overnight)	40 °C

S4: Discussion on the impact of different assumptions of the selective dissolution procedure.

The assumption (2) that crystalline slag phases don't react was confirmed by QXRD, where their content remained constant over time. Moreover, XRD on the residue after the selective dissolution

procedure of the blended cement with 70 wt% slag after 150 days hydration (fig. Sf2) showed that there was no significant dissolution of the crystalline phases in the selective dissolution solution.

Assumption (3), that all Mg of the slag leads to the formation of $Mg_5Al_2(OH)_{14}(CO_3)$, is a simplified view especially in these materials. The effect of different Mg/Al-ratios and different anions has been discussed in detail by Lumley et al.[18]. Additionally, it is known that Fe can substitute for Al in hydrotalcite [19], which may affect the calculation as well as the molar weight will change. Additionally, while hydrotalcite is typically expected to remain in the residue, no clear reflection due to this phase was observed in the residue of cement paste with 70 wt% slag at 150 days hydration (fig. Sf2). Only a small reflection due to another phase which was also present in the blended cement pastes could be observed, although with a much lower intensity than before the selective dissolution procedure. As discussed later, the full nature of this phase remains unclear at this point. Hence as this phase forms to a higher extent at later ages, this leads to further uncertainty of the reaction degree with higher replacement levels, especially at later ages. Neglecting this assumption, and thus assuming no hydrotalcite-like phase remains in the solution, yields a decrease of the reaction degree < 1 % absolute.

Assumption (4), i.e. that the unreacted NFM slag dissolves in the same way as the original, non-blended slag, during the selective dissolution can lead to about 7-10 % absolute increase in reaction degree if the related correction is disregarded. In reality it is likely that the most reactive part of the slag has already dissolved in the hydrated blends, especially at later ages, and thus the degree of reaction could be underestimated. Moreover, at early ages this assumption may affect the lower replacement levels more significantly, as the results from QXRD (fig 4 in the main text, table St 3) seem to indicate a higher reaction degree at 8 days for lower replacement levels. Hence as the most reactive part of the slag, in particular the smallest particles, already reacted for the lower replacement levels, it may dissolve less during the selective dissolution procedure and thus lead to more negative reaction degrees.

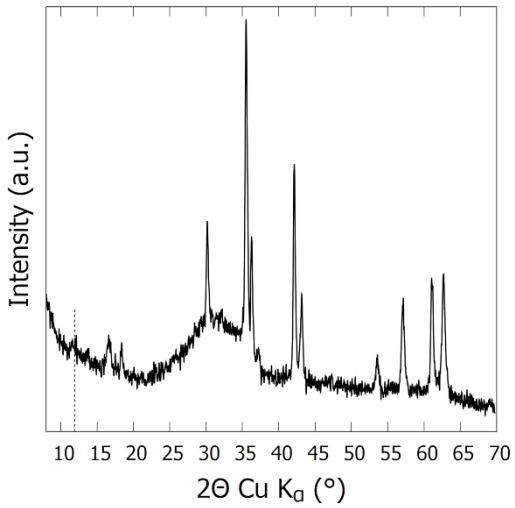

Figure Sf2: Diffraction pattern of the blended cement with 70 wt% slag hydrated for 150 days after selective dissolution with a NaOH-EDTA-TEA solution. The dotted line indicates the original position of the reflection due to a mössbauerite-like LDH in the blended cement paste before selective dissolution. The reflection around 16.9 ° 2Θ CuKα originates from the polycarbonate filter, the other strong reflections are due to the crystalline phases of the slag.

S5: Quantitative XRD results with different C-(A)-S-H structures and discussion of their effect on the slag reaction degree.

The reaction degree of the slag was also determined from QXRD using the PONKCS method (table St3). Whenever the C-(A)-S-H peak at d = 3.03 Å was adapted based on the diffraction pattern of each blended cement at 150 days, in order to account for the difference in C-(A)-S-H structure, there is a certain decrease in the reaction degree. As there was a clear misfit at later ages and higher replacement levels if this adaption was not used, the use of the adapted C-(A)-S-H peak most likely yields more accurate results. On the other hand, the significant overlap of the C-(A)-S-H structure and the amorphous part of the slag could also lead to parameter correlations which would reduce the accuracy. Hence here both the results of Rietveld analysis without and with the peak refinement are reported in table 4 as "CSH white cement" and "CSH blended cement" respectively in order to indicate a range of expected reaction degrees. At early age the C-(A)-S-H structure is expected to be more similar to that in the white cement aged for 7 years and the results from this refinement are more reasonable. On the other hand at later age the refined C-(A)-S-H structure should be more correct. However it should be noted that a small misfit could still be observed as a refinement of all the peaks of the C-(A)-S-H structure was not feasible due to clear parameter correlations with the Pawley phase used for the amorphous part of the slag. In all cases the effect of the type of C-(A)-S-H structure on the degree of hydration of the clinker phases is limited (< 5%), with the exception of C_2S which is always difficult to quantify due to extensive overlap with other phases. For the reaction degree of the slag, there is a systematic decrease of 5 to 10% in reaction degree when the C-(A)-S-H structure is refined on the hydrated blended cements at 150 days.

Table St3: Reaction degrees determined by selective dissolution (S.D.) and QXRD, using a C-S-H background structure based on 7-year old white cement [3] and after refinement of this structure using the diffractogram of blended cements after 150 days hydration.

		CSH white cement 7 years						CSH blended cement 150 days						S.D.[a]
		C_3S	C_2S	C_3A[b]	C_4AF	Am. Slag	Tot. Slag[c]	C_3S	C_2S	C_3A[c]	C_4AF	Am. Slag	Tot. Slag[c]	Slag
Slag (wt %)	Time (days)	DoH[d] (%)						DoH[d] (%)						DoH (%)
Est. Error (%) [20]		±5	±10	±10	±5		±10	±5	±10	±10	±5		±10	
	2	78	31	43	9	-	-	-	-	-	-	-	-	-
	8	87	35	63	24	-	-	-	-	-	-	-	-	-
0	28	90	44	75	34	-	-	-	-	-	-	-	-	-
	91	94	63	81	47	-	-	-	-	-	-	-	-	-
	150	93	64	81	49	-	-	-	-	-	-	-	-	-
	2	79	34	51	10	5	3	80	33	52	10	-7	-7.0	n.d.
	8	95	37	77	34	14	10	94	36	80	33	4	1	-7.3
30	28	96	55	91	45	22	17	96	54	90	44	16	12	6.0
	91	97	62	89	49	29	22	97	61	90	48	20	15	17.8
	150	97	71	91	55	40	33	97	70	90	54	32	25	23.2

	2	83	34	51	10	7	5	83	32	51	9	1	0	n.d.
	8	97	35	86	38	7	5	96	35	86	35	1	0	-1.6
50	28	99	52	94	54	23	19	99	50	90	52	18	15	9.0
	91	99	77	100	56	28	23	99	70	100	54	21	17	19.1
	150	98	75	90	59	32	26	98	68	92	57	25	20	25.1
	2	90	27	55	10	-3	-3	90	24	55	10	-7	-6	n.d.
	8	98	31	78	25	4	3	98	25	92	24	-2	-2	0.4
70	28	100	47	100	60	16	13	100	40	100	55	15	11	8.9
	91	100	66	100	68	23	19	99	55	100	65	20	16	19.4
	150	99	71	97	73	27	22	100	63	95	68	21	17	23.4

[a] based on the selective dissolution procedure with an NaOH-EDTA-TEA solution.
[b] C_3A was not always clearly visible at late ages (> 28 day), making accurate quantification difficult and likely causes the decrease in DoH at 150 days.
[c] Total slag content is calculated as the sum of the quantities of amorphous slag content, wüstite and magnetite obtained from the Rietveld analysis.
[d] DoH = degree of hydration.

S6: Figure showing the Fe/Ca vs Si/Ca molar ratio in the inner product obtained by SEM-EDX using point analysis.

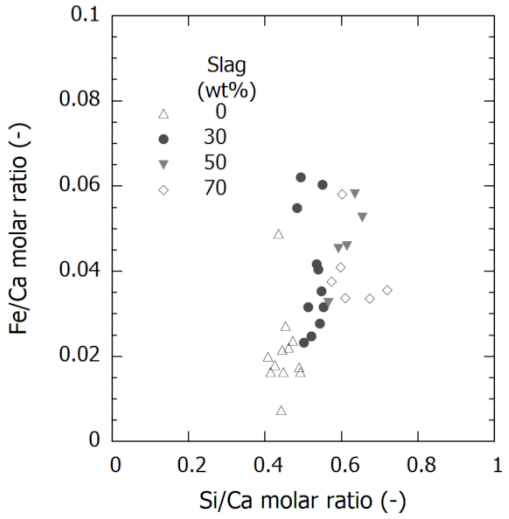

Figure Sf3: Fe/Ca vs Si/Ca atomic ratios obtained by SEM-EDX using point analysis, selecting points in the inner product of the cement pastes with different replacement of PC by NFM slag after 91 days of hydration.

S7: Figure showing the Fe/Ca vs Si/Ca molar ratio in the inner product obtained by SEM-EDX using point analysis.

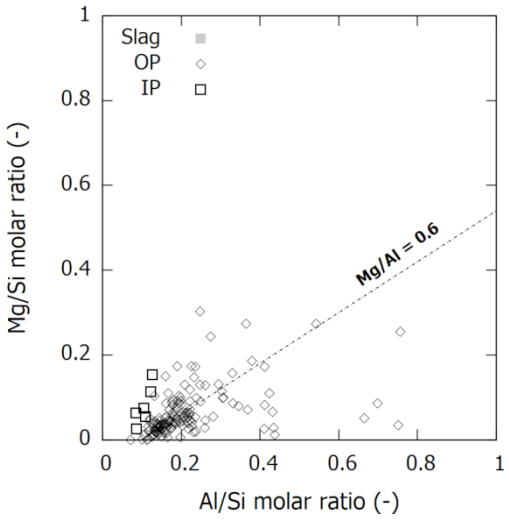

Figure Sf4: : Mg/Si vs Al/Si atomic ratios obtained by SEM-EDX using point analysis on points in the binder of the blended cement paste with 70 wt% slag.

S8: Table of the pore solution concentrations

Table St4: Concentrations of main elements in the pore solution of neat PC and cement blended with NFM slag.

Slag (wt%)	Time (days)	Na	K	Ca	Al (mmol/l)	Si	S	Fe	OH^- [a]	pH (-)	C.B.E.[b] (%)
	2	141[c]	305[c]	3.7	0.08	0.22	6.8	n.d.	471	13.6	-7
	8	206	389	4.2	0.09	0.26	11	n.d.	468	13.6	19
0	28	233	424	1.9	0.13	0.34	11	n.d.	n.d.[d]	n.d.[d]	n.d.
	91	243[c]	403[c]	3.1	0.16	0.21	26[c]	0.007	n.d.[d]	n.d.[d]	n.d.
	2	109	206	4.6	0.07	0.14	1.2	n.d.	301	13.4	6
	8	176[c]	253[c]	4.5	0.07	0.13	2.3	n.d.	420	13.6	3
30	28	302[c]	316[c]	7.5	0.09	0.26	5.0	n.d.	432	13.6	30
	91	285[c]	241[c]	2.6	0.22[c]	0.22	12	0.012	425	13.6	9
	2	98[c]	161[c]	6.5	0.06	0.18	0.94	n.d.	217	13.3	19
	8	156	176	5.0	0.09	0.12	1.0	n.d.	322	13.5	5
50	28	232	182	2.5	0.24	0.17	1.9	n.d.	308	13.4	23
	91	268[c]	151[c]	2.0	0.44[c]	0.25	6.3	0.010	330	13.4	15
	2	66	91	9.8	0.03	0.06	0.32	n.d.	161	13.2	7
	8	119	109	5.1	0.11	0.09	0.33	n.d.	211	13.3	6
70	28	266[c]	284[c]	3.5	0.14	0.20	6.1	n.d.	402	13.6	26
	91	236[c]	88[c]	1.3	0.84[c]	0.44	6.0	0.007	264	13.4	13
	D.L.[e]	$1e^{-2}$	$1e^{-2}$	$6e^{-3}$	$4e^{-5}$	$4e^{-4}$	$1e^{-3}$	$4e^{-5}$			

[a] Calculated from the pH measurements using ionic strengths from GEMS [21, 22] and the Helgeson form of the Debye-Hückel equation [23, 24] to calculate the activity coefficient.
[b] Charge balance error, calculated as the ratio of the difference in total charge due to cations (Na^++K^++2·Ca^{2+}) versus anions (OH^- + 2·S^{2-}) to the total charge caused by the cations.
[c] Measured concentration > highest standard measured due to a dilution error where a lack of material prevented repeated measurement of the samples. Based on the measurements without this dilution error, the expected maximum error is < 7% for Na and K.
[d] Not enough pore solution could be obtained to measure pH and calculate OH^- concentrations but no significant changes are expected at later ages [25]
[e] detection limits for 2-28 days, at 91 days the detection limits are 10 times lower as there was less dilution.

Table St5: Concentrations of some relevant trace elements in the pore solution of neat PC and cement blended with NFM slag.

Slag (wt%)	Time (days)	Cr	Cu	P	Pb	Zn
				(mmol/l)		
	2	0.08	0.003	0.006	$2e^{-4}$	$9e^{-4}$
	8	0.14	0.004	0.009	$3e^{-4}$	0.001
0	28	0.14	0.014	0.05	$4e^{-4}$	0.007
	91	0.16	0.003	0.04	$4e^{-4}$	0.002
	2	0.03	0.004	0.002	$2e^{-4}$	$7e^{-4}$
	8	$4e^{-4}$	$1e^{-4}$	0.007	$2e^{-5}$	$9e^{-4}$
30	28	$8e^{-4}$	$5e^{-4}$	0.005	$3e^{-5}$	0.003
	91	$6e^{-5}$	$9e^{-5}$	0.012	$2e^{-5}$	0.002
	2	0.01	0.007	0.001	$2e^{-4}$	0.003
	8	$5e^{-5}$	$7e^{-5}$	0.005	$2e^{-5}$	0.002
50	28	$7e^{-5}$	$2e^{-4}$	0.017	$2e^{-5}$	0.002
	91	< D.L.	$7e^{-5}$	0.005	$7e^{-6}$	0.002
	2	0.001	0.002	0.002	$2e^{-4}$	$5e^{-4}$
	8	< D.L.	$3e^{-4}$	0.003	$2e^{-5}$	$7e^{-4}$
70	28	< D.L.	$2e^{-4}$	0.012	$2e^{-5}$	0.002
	91	< D.L.	$1e^{-4}$	0.005	$1e^{-5}$	0.002
	D.L.[e]	$4e^{-5}$	$7e^{-6}$	$8e^{-4}$	$9e^{-7}$	$6e^{-5}$

S9: Table of the effective saturation indices

Table St6: Effective saturation indices for ettringite (Ett.), gypsum, strätlingite (Str.), C-S-H, Ca(OH)2 (CH), siliceous hydrogarnet (Si-Hg), ferrihydrite (Fh), hemicarboaluminate (Al-Hc), monocarboaluminate (Al-Mc), hemicarboferrite (Fe-Hc) and monocarboferrite (Fe-Mc).

Slag (wt%)	Time (days)	Ett.	Gypsum	Str.	C-S-H	CH	Hdg	Fh	Al-Hc	Al-Mc	Fe-Hc	Fe-Mc
	2	0.28	-1.04	-0.74	0.47	0.25	-	-	0.002	0.20	-	-

	8	0.34	-0.92	-0.71	0.51	0.26	-	-	0.02	0.22	-	-
0	28	0.22	-1.10	-0.71	0.40	0.14	-	-	-0.05	0.15	-	-
	91	0.39	-0.81	-0.66	0.42	0.21	0.58	-1.07	0.03	0.23	0.07	0.25
	2	0.20	-1.23	-0.74	0.38	0.20	-	-	-0.01	0.19	-	-
	8	0.22	-1.20	-0.76	0.41	0.25	-	-	0.01	0.21	-	-
30	28	0.38	-0.94	-0.64	0.61	0.33	-	-	0.10	0.28	-	-
	91	0.33	-0.97	-0.62	0.38	0.17	0.61	-0.92	0.02	0.23	0.09	0.27
	2	0.24	-1.14	-0.69	0.42	0.19	-	-	-0.009	0.19	-	-
	8	0.21	-1.27	-0.71	0.38	0.22	-	-	0.02	0.22	-	-
50	28	0.19	-1.28	-0.61	0.31	0.11	-	-	-0.004	0.21	-	-
	91	0.28	-1.10	-0.53	0.33	0.08	0.57	-0.90	0.01	0.23	0.01	0.20
	2	0.19	-1.20	-0.83	0.27	0.20	-	-	-0.04	0.16	-	-
	8	0.15	-1.40	-0.68	0.27	0.15	-	-	0.002	0.21	-	-
70	28	0.30	-1.04	-0.66	0.42	0.21	-	-	0.02	0.22	-	-
	91	0.23	-1.17	-0.43	0.31	-0.04	0.50	-0.93	-0.03	0.20	-0.11	0.09

References

[1] Young, J. C., & Finn, A. N. Effect of composition and other factors on the specific refraction and dispersion of glasses. J. Res. Nat. Bur. Stand 25 (1940) 759-782.

[2] N.V.Y. Scarlett, I.C. Madsen, Quantification of phases with partial or no known crystal structures, Powder Diffraction 21 (2006) 278-284. https://doi.org/10.1154/1.2362855.

[3] X. Li, R. Snellings, K.L. Scrivener, Quantification of amorphous siliceous fly ash in hydrated blended cement pastes by X-ray powder diffraction, J. Appl. Cryst. 52 (2019) 1358-1370. https://doi.org/10.1107/S1600576719013955.

[4] A.G. De La Torre, S. Bruque, J. Campo, M.A.G. Aranda, The superstructure of C_3S from synchrotron and neutron powder diffraction and its role in quantitative phase analysis, Cem. Concr. Res. 32 (2002) 1347-1356. https://doi.org/10.1016/S0008-8846(02)00796-2.

[5] M.N. de Noirfontaine, F. Dunstetter, M. Courtial, G. Gasecki, M. Singnes-Frehel, Polymorphism of tricalcium silicate, the major compound of Portland cement clinker 2. Modelling alite for Rietveld analysis, an industrial challenge, Cem. Concr. Res. 36 (2006) 54-64. https://doi.org/10.1016 / j.cemconres.2004.12.004.

[6] W.G. Mumme, L. Cranswick, B. Chakoumakos, Rietveld Crystal Structure Refinement from High Temperature Neutron Powder Diffraction Data for the Polymorphs of Dicalcium Silicate, Neues Jahrb. für Mineral. Abhandlungen, 170 (1996) 171-188. http://hdl.handle.net/102.100.100/230393?index=1

[7] W.G. Mumme, R.J. Hill, G.W. Bushnell, E.R. Segnite, Rietveld Crystal Structure Refinements, Crystal Chemistry and Calculated Powder Diffraction Data for the Polymorphs of Dicalcium Silicate and Related Phases, Neues Jahrb. für Mineral. Abhandlungen 169 (1995) 35-68. http://hdl.handle.net/102.100.100/234637?index=1.

[8] P. Mondal, J.W. Jeffery, The Crystal Structure of Tricalcium Aluminate, $Ca_3Al_6O_6$, Acta Cryst. B 31 (1975) 689-697. https://doi.org/10.1107/S0567740875003639.

[9] F. Nishi, Y. Takeuchi, The Al6O18 Rings of Tetrahedra in the Structure of $Ca_{8.5}NaAl_6O_{18}$, Acta Cryst. B 31 (1975) 1169-1173. https://doi.org/10.1107/S0567740875004736.

[10] Y. Takeuchi, F. Nishi, I. Maki, Crystal Chemical Characterisation of the (CaO)3·Al2O3-Na2O Solid-Solution Series, Z. Kistallogr. Cryst. Mater. 152 (1980) 259-307. https://doi.org/10.1524/zkri.1980.152.14.259.

[11] A.A. Colville, S. Geller, The crystal structure of brownmillerite, Ca_2FeAlO_5, Acta Cryst. B27 (1971) 2311-2315. https://doi.org/10.1107/S056774087100579X.

[12] W.R. Busing, H.A. Levy, Neutron Diffraction Study of Calcium Hydroxide, J. Chem. Phys., 26 (1957) 563. https://doi.org/10.1063/1.1743345.

[13] F. Goetz-Neunhoeffer, J. Neubauer, Refined Ettringite (Ca6Al2(SO4)3(OH)12.26H2O) Structure for Quantitative X-Ray Diffraction Analysis, Powder Diffr. 21 (2006) 4-11. https://doi.org/10.1154/1.2146207.

[14] T. Runcevski, R.E. Dinnebier, O.V. Magdysyuk, H. Pöllmann, Crystal Structures of Calcium Hemicarboaluminate and Carbonated Calcium Hemicarboaluminate from Synchrotron Powder Diffraction Data, Acta Cryst. B 68 (2012) 493-500. https://doi.org/10.1107/S010876811203042X.

[15] M. Francois, G. Renaudin, O. Evrard, A Cementitious Compound with Composition $3CaO·Al_2O_3$ $CaCO_3·11H_2O$, Acta Cryst. C 54 (1998) 1214-1217. https://doi.org/10.1107/S0108270198004223.

[16] M. Bellotto, B. Rebours, O. Clause, J. Lynch, D. Bazin, E. Elkaïm, A Reexamination of Hydrotalcite Crystal Chemistry, J. Phys. Chem. 100 (1996) 8527-8534. https://doi.org/10.1021/jp960039j.

[17] B.Z. Dilnesa, B. Lothenbach, G. Renaudin, A. Wichser, D. Kulik, Synthesis and characterization of hydrogarnet $Ca_3(Al_xFe_{1-x})_2(SiO_4)_y(OH)_{4(3-y)}$, Cem. Concr. Res. 59 (2014) 96-111. https://doi.org/10.1016/j.cemconres.2014.02.001.

[18] J.S. Lumley, R.S. Gollop, G.K. Moir, H.F.W. Taylor, Degrees of reaction of the slag in some blends with Portland cements, Cem. Concr. Res. 26 (1996) 139-151. https://doi.org/10.1016/0008-8846(95)00190-5.

[19] K. Rozov, U. Berner, C. Taviot-Gueho, F. Leroux, G. Renaudin, D. Kulik, L.W. Diamond, Synthesis and characterization of the LDH hydrotalcite-pyroaurite solid-solution series, Cem. Concr. Res. 40 (2010) 1248-1254. https://doi.org/10.1016/j.cemconres.2009.08.031.

[20] K.L. Scrivener, T. Füllmann, E. Gallucci, G. Walenta, E. Bermejo, Quantitative study of Portland cement hydration by X-ray diffraction/Rietveld analysis and independent methods, Cem. Concr. Res. 34 (2004) 1541-1547. https://doi.org/10.1016/j.cemconres.2004.04.014.

[21]T. Wagner, D.A. Kulik, F.F. Hingerl, S.V. Dmytrieva, GEM-Selektor geochemical modelling package: TSolMod Library and data interface for multicomponent phase models, Can. Mineral. 50 (2012) 1173-1195. https://doi.org/10.1007/s10596-012-9310-6.

[22] D.A. Kulik, T. Wagner, S.V. Dmytrieva, G. Kosakowski, F.F. Hingerl, K.V. Chudnenko, U.R. Berner, GEM-Selektor geochemical modeling package: revised algorithm and GEMS3K numerical kernel for coupled simulation codes, Comput. Geosci. 17 (2013) 1-24. https://doi.org/10.1007/s10596-012-9310-6.

[23] H.C. Helgeson, D.H. Kirkham, G.C. Flowers, Theoretical prediction of the thermo- dynamic behavior of-aqueous electrolytes at high pressures and temperatures: IV. Calculation of activity coefficients, osmotic coefficients, and apparent molal and standard and relative partial molal properties to 600C, Am. J. Sci. 281 (1981) 1249-1516. https://doi.org/10.2475/ajs.281.10.1249.

[24] P. Debye, E. Huckel, (1923) “Zur Theorie der Elektrolyte”, Z. Phys., 24, 185-206.

[25] A. Vollpracht, B. Lothenbach, R. Snellings, J. Haufe, The pore solution of blended cements: A review, Mater. Struct. 49 (2016) 3341-3367. https://doi.org/10.1617/s11527-015-0724-1.